CHINESE JOURNAL OF PHYSICS VOL. 37, NO. 5 OCTOBER 1999

Determinism Test, Noise Estimate and Hidden E'requency Recognition: the Singular Value Decomposition Approach

Jing-Yuan Ko, Jiann-Shing Lih, Ming-Chung Ho,
Charng-Ching Tsai, and Jyh-Long Chern
Nonlinear Science Group, Department of Physics, National Cheng Kung University, Tainan, Taiwan 701, R.O.C.
(Received January 6,1999)

Given a scalar time series, the trajectory matrix of a system can be constructed by the Takens' delay-coordinate map theorem. We employ the method of singular value decomposition (SVD) to derive the eigenvalue spectrum of the trajectory matrix. It is shown that when the embedding dimension of the trajectory matrix is very large, the SVD eigenvalue spectrum could be utilized to test the determinism and estimate the strength of noise in time series. On the other hand, we show that the dynamically connected frequency components hidden in chaotic time series can be detected by the SVD method. Finally, three kinds of circuit experiments are presented as demonstrations.

PACS. 05.45.+b – Theory and the models of chaotic systems.

I. Introduction

Progress in nonlinear dynamics has stimulated general interest on complex phenomena. The study of chaos becomes a paradigm in nonlinear studies. The fundamental nature of chaos is determinism. But, how does one go about recognizing the determinism in a complex time series? In 1990, Sugihara and May considered the prediction ability inherent in chaos for measuring the deterministic dynamics in a time series [1]. On the other hand, Kaplan and Glass measured the average directional vectors in the coarse-grained dimensional space for testing [2]. Later, Wayland *et al.* simplified the approach of Kaplan and Glass by employing the inherent property of a deterministic time series in phase space, i.e., the continuity of trajectory [3]. Both works of Kaplan-Glass and Wayland et *al.* suggested that the continuity in an embedded phase space is enough for extracting the determinism in a time series. Furthermore, Salvino and Cawley indicated that continuity still holds even for many arbitrary vector fields over an attractor and a unique feature associated with an optimum average over a wide range of time delay could be employed as a novel test for determinism [4]. Thus far, it is well accepted that phase space continuity can be used as a test of determinism for continuous-time dynamical systems. Unfortunately, there remains a practical task in such a determinism test, i.e., the criterion of the ball size in averaging is not available in general.

Let us turn to consider another important subject in the study of chaos, i.e., the applicability of chaos. Usually, power spectrum analysis is the first tool to gain dynamical information [5]. In many real situations, only one physical variable can be observed. However, the intrinsic nature of dynamical systems could be multivariate. Hence, in such situations it is of practical importance to develop a technique that provides access to the whole spectrum of frequency components inherent in a dynamical system. Recently, Ortega introduced a procedure in response to the above challenge [6]. The essence of Ortega's idea is to embed the data in multidimensional space with some unit cell balls and record the density of the points that the trajectory met with the cell as it evolves. By taking a power spectrum analysis on this density flow, more dynamically connected frequency components in a continuous time dynamical system can be extracted. Again, for this method it is essential to have an "*appropriate*" ball size in phase space for determining the density flow. This leads to a serious problem of flexibility and efficiency in applications, which is exactly the same problem as that for the case of determinism test mentioned above.

The SVD method has been useful in extracting qualitative dynamics from experiment data as shown by Broomhead and King [7]. Typical example is to calculate the correlation dimension of an attractor [8]. On the other hand, Brown *et al.* [9] and Stoop and Parisi [10] also advocated its advantage to restrict the dynamics to the tangent plane of the attractor prior to approximating the local dynamics. In the field of noise reduction, the SVD method has also been employed to enhance the accuracy of local linear dynamics [11, 12]. In this paper, we will present the advantages of the SVD approach in testing determinism, estimating the noise strength, and recognizing the hidden frequency components in a time series. It should be noted that the support to our previous work [13] on determinism test is numerical simulations only. Thus, some important factors of the underlying working principle and limitation remain to clarify. In Sec. II we will briefly outline the general formalism of the SVD method presenting new geometric and algebraic interpretations such that the essential mechanism can be greatly illustrated. In Sec. III, we will show how to obtain the eigenvalue spectrum to test the determinism of a variety of time series. In Sec. IV, we will demonstrate how to estimate the noise level of a time series mixed with a uniform noise. A simple formula to deduce noise strength from time series will be attached. Furthermore, the silent features of the SVD approach associated with the length of time series, time delay, and embedding dimension, will be further appended as a complete illustration. In Sec. V, the SVD method will be used in tandem with phase space reconstruction to detect the dynamically connected frequency components hidden in a chaotic time series [14]. In Sec. VI we will present the circuit experiments as an exploration of estimating the noise level. Finally, in Sec. VII, concluding comments will be offered.

II. The SVD method: general formalism and its interpretation

II-1. General formalism

We assume that the dynamical system is described by a set of differential equations $\frac{dx}{dt} = \mathrm{F(X)}$ where $\mathrm{X} = (x_1, x_2, x_3, \ldots)$ represents the state vector. If physically one variable ν, say $\nu = x_1$ is measured, then we can have a time series $\{\nu(\Delta t), \nu(2\Delta t), \nu(3\Delta t), \ldots, \nu((N+d)\Delta t)\}$ where At is the time difference between two successive measurements, $(N+d)$ is the total number of data points, and d is the embedding dimension. Based on the Takens'

delay-coordinate map theorem [15], we can reconstruct a d-dimensional vector Y_i and define an N x a! trajectory matrix

$$A = \begin{bmatrix} Y_1 \\ Y_2 \\ \cdot \\ Y_N \end{bmatrix} = \begin{bmatrix} \nu(\tau) & \nu(2\tau) & \cdot & \nu(d\tau) \\ \nu(2\tau) & \nu(3\tau) & \cdot & \nu((d+1)\tau) \\ \cdot & \cdot & \cdot & \cdot \\ \nu(N\tau) & \nu((N+1)\tau) & \cdot & \nu((N+d-1)\tau) \end{bmatrix} \quad (1)$$

which contains all dynamical information. In above reconstruction, we have presumed the embedding dimension of an attracting manifold within the phase space to be d.

By using the SVD method, the matrix A *can* be decomposed as $A = VSU^T$ where V is an N x d orthogonal matrix, U is an d x d orthogonal matrix, and S is an d x d diagonal matrix. Meanwhile, $(V^TV)I_{i,j}=\delta_{ij}, (U^TU)I_{i,j}=(UU^T)I_{i,j}=\delta_{ij}$ and $S_{ij}=\delta_{ij}s(i)$ $(i=1,2,\ldots)$. The matrix S is the singular value matrix of A and s(i) is its corresponding singular value. Since $U^T(A^TA)U = S^2$ and $(A^TA)U = S^2U, [s(i)]^2$ *are* the eigenvalues of (A^TA) and correspondingly, U is the set of eigenvectors. We rearrange the normalized $[s(i)]^2$ in a descending order and name it as the SVD spectrum. The distribution of the eigenvalues (the SVD spectrum) could be utilized for testing determinism and estimating noise strength, as to be fully addressed below. Because U is an orthogonal matrix, its eigenvectors $U_i(i=1,2,\ldots,\mathrm{d})$ can be the orthogonal basis of the reconstructed phase space. The projected variables are $c_i(k) = AU_i$, where $k = 1,2,\ldots,N$ indicates time flow. Although U_i are not the eigenvectors of the matrix A, the flexibility and suitability of projected variables c_i can be established. The time flow of these reconstructed variables c_i and their spectrum characteristics could be utilized in recognizing the hidden frequency components in a chaotic time series, as also to be illustrated systematically below.

It should be noted that the use of the SVD projection method has been classified into two kinds of scheme [10], i.e., "global" and "local", according to whether the principal direction of the reconstructed attractor is "global" or "local". Here, the SVD approach is essentially a global one. It should be also noted that in our numerical simulation, we take a fourth-order Runge-Kutta algorithm to integrate the equations with a time step τ. In detecting the hidden frequencies, a small At is necessary. For simplicity, we will also let At $=\tau$ and employ a common FFT algorithm to estimate the power spectrum.

11-2. **Geometrical picture**

Let us first provide an intuitive illustration for the (global) SVD scheme. The SVD method is to explicitly construct the orthonormal bases of the nullspace and the range of a singular matrix. Specifically, the columns of V form an orthonormal set of basis vectors that spans the range. The number of these basis vectors is the same as the number of nonzero elements of s_i. Meanwhile, the columns of U form an orthonormal set of basis vectors that span the nullsapce. The number of these basis vectors is equal to the number of zero elements of s_i plus the number of free parameters of a singular matrix. In other words, when we applied the SVD algorithm to a trajectory matrix, which is a singular matrix, the number of nonzero elements of s_i is the degree of freedom for describing the dynamical system, which is defined by the trajectory matrix.

A simple interpretation of the SVD algorithm can be geometrically illustrated as shown below. Assume that the final state of a system is a fixed point, say (1.0, 2.0) in

a two-dimension phase space. For a simple illustration, only three successive states are considered, thus the trajectory matrix is $\begin{bmatrix} 1.0 & 2.0 \\ 1.0 & 2.0 \\ 1.0 & 2.0 \end{bmatrix}$. By using the SVD method, we solve the matrix and obtain the diagonal matrix $S = \begin{bmatrix} 3.87 & 0.00 \\ 0.00 & 0.00 \end{bmatrix}$, where the number of nonzero diagonal elements is 1. This is consistent with the degree of freedom required for embedding the fixed point. It can be shown that an extension to the case of n-dimensional phase space simply results in one nonzero diagonal element.

II-3. Algebraic interpretation

Let us now treat the SVD method with an algebraic point of view. By definition, the SVD method is essentially to solve the eigenvalue problem $(A^T A)U = S^2 U$, where

$$A^T A = \begin{vmatrix} \sum_{i=1}^{N} \nu(i\tau)\nu(i\tau) & \sum_{i=1}^{N} \nu(i\tau)\nu((i+1)\tau) & \cdots & \sum_{i=1}^{N} \nu(i\tau)\nu((i+d-1)\tau) \\ \sum_{i=1}^{N} \nu((i+1)\tau)\nu(i\tau) & \sum_{i=1}^{N} \nu((i+1)\tau)\nu((i+1)\tau) & \cdots & \sum_{i=1}^{N} \nu((i+1)\tau)\nu((i+d-1)\tau) \\ \sum_{i=1}^{N} \nu((i+d-1)\tau)\nu(i\tau) & \sum_{i=1}^{N} \nu((i+d-1)\tau)\nu((i+1)\tau) & \cdots & \sum_{i=1}^{N} \nu((i+d-1)\tau)\nu((i+d-1)\tau) \end{vmatrix} \quad (2)$$

The matrix $A^T A$ is a symmetric real matrix and its elements are the time-delay correlation of the time series $\{\nu(t)\}$. Thus, we should consider a variety of correlation forms satisfied a D x D symmetric real matrix, i.e.,

$$A^T A = \begin{bmatrix} f(0) & f(1) & \cdots & f(D-1) \\ f(1) & f(0) & \cdots & f(D-2) \\ \cdot & & & \\ f(D-1) & f(D-2) & \cdots & f(0) \end{bmatrix} \quad (3)$$

where f is the correlation function. Let us suppose the elements fit an exponential decay form, $f(x) = e^{-bx}$, which may simulate a chaotic time series. Next, we solve the eigenvalues of the matrix $A^T A$ numerically and rearrange the eigenvalues with a descent order, i.e., λ_n (n = $1, 2, \ldots, D$) and $\lambda_1 > \lambda_2 > \cdots > \lambda_D$. It is found that the eigenvalues follow

$$\lambda_n \approx \frac{\alpha(b)}{D} e^{-\alpha(b)n}, \quad (4)$$

where $\alpha(b) \approx 9.7e^{-b}$. This is essentially an exponential decay. On the other hand, for a uniform white noise, its time-delay satisfies correlation $f(z) = S(z)$, and the eigenvalues of $A^T A$ are all equal to 1. Thus, the eigenvalue spectrum for a uniform noise does not decline but to maintain a constant level.

III. Determinism test

III-1. Deterministic signals

In this section, we show how to utilize the SVD method for testing determinism. Specifically, the reconstructed vectors are used to form a trajectory matrix. By using the SVD method, a set of orthogonal vectors can be derived from the trajectory matrix and the eigenvalues will form the SVD spectrum. We also employ the Takens' delay-coordinate map theorem for reconstructing phase space, but the embedding dimension has been set to be very large.

For a trajectory matrix which represents a high-dimensional object, a large part of the eigenvalues will not vanish. This idea suggests that for an uncorrelated stochastic source whose dimension is intrinsically infinite, its eigenvalues will never become zero regardless the size of embedding dimension. Hence, the SVD eigenvalue spectrum for a white noise should be flat and not zero. Figure l(a) and (b) show the SVD spectra of a uniform white noise and a Guassian white noise. Both spectra are flat and they are almost identical. This is reasonable because these two stochastic sources exhibit the same homogeneity character in all directions of phase space. On the other hand, for a periodic signal, sin(t), and a qusiperiodic signal, sin(t) t $\sin(\sqrt{2}t)$, whose SVD spectra are presented by Fig. l(c) and (d), the corresponding eigenvalues drop rapidly as the index of dimension increased. The appearance of sudden drop is a typical feature for the regular signals with sharp spectra and it can be expected based on the geometric consideration outlined above. For the chaotic signal, the characteristics should be different as discussed in Sec. II(C). We take the Lorenz model which follows $\frac{dx}{dt} = \sigma(y-x)$, $\frac{dy}{dt} = rx - y - xz$, $\frac{dz}{dt} = xy - bz$, where $\sigma = 10.0$, $r = 28.0$ and $b = 2.66$, as an illustration. The step size is 0.005 and the data length is 5100. We take the variable x as the variable for reconstruction. As one can see from Fig. l(e), the eigenvalues displays an exponential decay. The decay rate can be estimated using $[s(l)]^2 \propto \exp[-\gamma l]$, and γ = 1.50 for the Lorenz model. This exponential decay is a general signature of chaos in the SVD spectrum, though the value of decay rate depends the size of the embedding dimension and the model itself. Indeed, the other typical models, such as the Rossler chaos, FIR-NH_3 model, and so on, have been explored and exactly the same features have been numerically demonstrated [13].

Although an algebraic interpretation is given in Sec. II(C), the origin of this non-sudden drop characteristic in SVD eigenvalue spectrum for the chaotic attractor can be figured out differently. Substantially, the SVD algorithm seeks for a complete set of orthogonal base vectors whose total number is strictly an integer. However, chaotic attractors are all of non-integer dimension. Thus, the resulting fractional value of dimension of the attractor should distribute over to the rest of SVD dimension index.

111-2. Surrogate tests

It is important to perform the surrogate test to ensure the determinism nature identified and explored by the SVD method. To check the deterministic nature further, we follow the prescription of Pierson and Moss [16] to destroy the sequential order to form a surrogate set and reanalyze the SVD spectrum. We also follow Ref. [17] and use the unwindowed Fourier transform algorithm to generate the surrogate data. As shown in Fig. 2, where the Lorenz model is used as a typical example, the SVD spectra of the surrogate data are

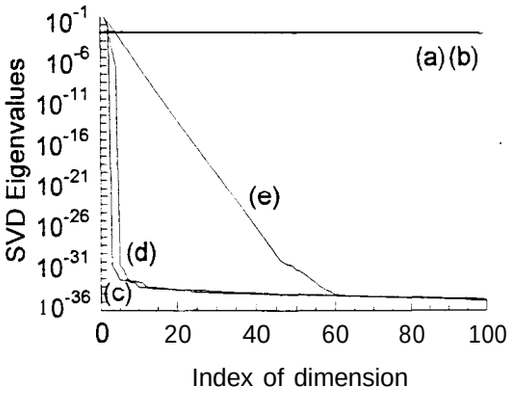

FIG. 1. The SVD eigenvalue spectra of seven different signals, (a) uniform white noise, (b) Gaussian white noise, (c) a periodic signal, sin(t), (d) a quasiperiodic signal, sin(t) $+\sin(\sqrt{t})$, (e) the Lorenz model.

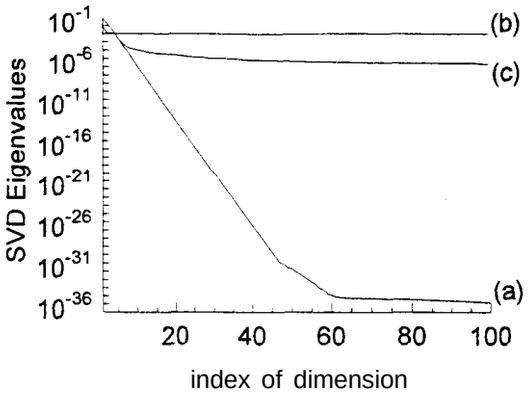

FIG. 2. The SVD eigenvalue spectra of a time series from the Lorenz model and its surrogate data. (a) is the original time series, (b) is generated by randomizing the sequential order of the original time series, and (c) is obtained by the unwindowed Fourier transformation algorithm.

completely different from the original one. In short, deterministic nature can be extracted based on the SVD eigenvalue spectrum.

111-J. Stochastic signals

We demonstrate the analysis with the models driven by dynamical noise as following. First, we take the equation $\frac{dx}{dt}$ = sint $+\alpha\eta(t)$, where α is the noise strength and $\eta(t)$ is the Gaussian white noise. In Fig. 3(a) the corresponding SVD spectrum shows a sudden drop when $\alpha = 10^{-10}$. As a large $\alpha = 10^{-1}$, the slow-inclination of the SVD spectrum is lifted. Next, we take the noisy Duffing oscillator, $\frac{d^2x}{dt^2}$ • t $a\frac{dx}{dt} - x + x^3 = f\sin wt$ t on(t) where a = 0.25, $f = 0.4$, $w = 1.0$ as an example. The result is shown by Fig. 3(b). One can see the exponential-decay feature persist. To show the generality, we present another case, a modified Lorenz model for which the change of y component follows $\frac{dy}{dt} = rx - y - xz + \alpha\eta(t)$. The result is shown in Fig. 3(c) where similar feature can be identified. In addition, the lifted slow-inclination is another general feature of the SVD spectrum for the increasing strength of noise.

IV. Noise estimate

IV-l. Simple test

The appearance of slow-inclination is a general feature of the SVD eigenvalue spectrum. In other words, at the end of the exponential drop of the SVD spectrum, a turning

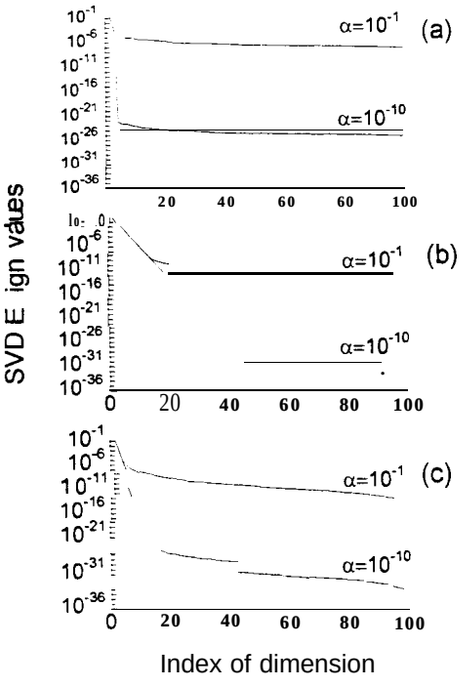

FIG. 3. The SVD eigenvalue spectra for different stochastic models. In these cases, the small noise strength is $\alpha = 10^{-10}$, and the large noise strength is $\alpha = 10^{-1}$. (a) A periodic solution with noise, (b) the noisy chaotic Duffing oscillator, and (c) the noisy chaotic Lorenz model.

point occurs at the dimension index $l = l_c$. As an example, see the Lorenz model shown in Fig. 1. After this point a flat floor takes place around 10^{-35} which is most likely due to the intrinsic numerical noise. This slow-inclination forms another essential part of the SVD eigenvalue spectrum. To explore the underlying feature caused by the noise, we add a Gaussian white noise whose standard deviation is σ to the x variable of the Lorenz model. We define the ratio between the noise strength and the time series as R.

$$R = \frac{2\sigma}{x_{\max} - x_{\min}}, \tag{5}$$

where $x_{\max}$ and $x_{\min}$ are the maximum and the minimum value of the data x respectively. As shown in Fig. 4, for $R < 1$, the decay rate does not change while the slow-inclination of the spectrum shift up/down proportionally. Owing to the slope of this slow-inclination is -0.014 $\pm$ 0.001, we define the interception f as the noise level of the slow-inclination. In Fig. 5, different values of R hold a relation

$$f = cR^{\delta} \tag{6}$$

for a large range R from 10^{-11} to 10^{-1} where f is the corresponding noise level, c is about 0.02 and δ is about 1.98. Nevertheless, the deviation occurs for $R \sim 1.0$ (as shown in the figure inset).

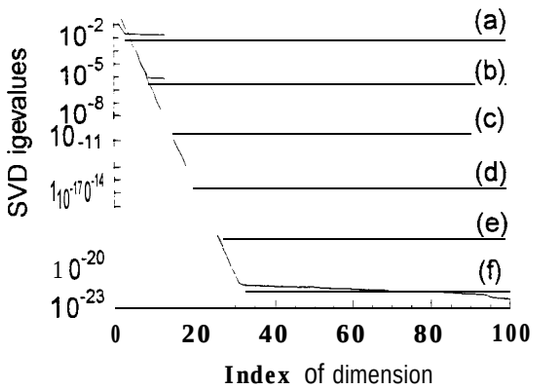

FIG. 4. The SVD eigenvalue spectra for the Lorenz model with different levels of added uniform noise where the noise contamination factor $\boldsymbol{R}$ = (a) 1.0, (b) 10^{-2}, (c) 10^{-4}, (d) 10^{-6}, (e) 10^{-8} and (f) 10^{-10}.

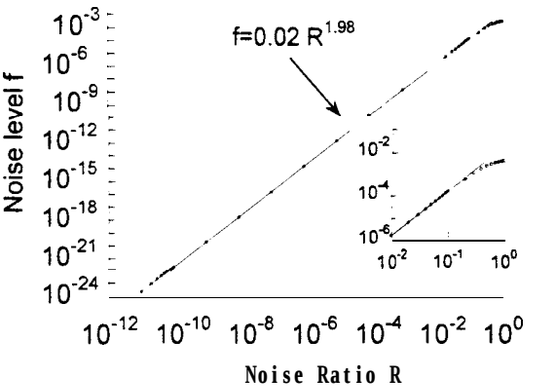

FIG. 5. The noise level f versus the observational Gaussian noise ratio $\boldsymbol{R}$. The line is $f = 0.02\ R^{1.98}$. The inset is the magnified of portion of the noise level for $\boldsymbol{R} \sim 1$.

IV-2. Estimate formulate

We have **tested** the generality. It is found that the exponent δ is equal to **2.00 ± 0.02** for a variety of signals, such as the Lorenz chaos, the Rossler chaos, the FIR-NH_3 laser model and even sine signal. For the Lorenz model, c = 1.07 x 10^{-2} while for the FIR-NH_3 laser model, c = 1.64 x 10^{-2} and for the Rossler chaos, c = 0.80 x 10^{-2}[13]. Thus, for a chaotic time series, one can estimate the noise level f. This means that by using the relation

$$f = cR^2 \sim \mathbf{0.01}\ R^2, \tag{7}$$

one can deduce the value of R which roughly represents the strength of the noise contained in real time series. We note that the R-value only indicate a relative ratio of noise strength. To estimate absolute noise strength I_N, the intensity of a measured time series, I_t, should be evaluated first. Then we have

$$I_N = \frac{RI_t}{R+1}. \tag{8}$$

According to the results shown above, one can approximately estimate the noise level for any time series. We note that the constant c $\approx$ 0.01 can be employed without the loss of too much generality. Therefore, Eq. (7) turns out to be a useful estimate.

IV-3. Influences of data length, time delay, and embedding dimension

Next, we use the Lorenz model to explore the silent features of the SVD analysis. namely the length of time series, time delay, and embedding dimension. Different models.

such as the Duffing oscillator and the Van der Pol oscillator, have also been tested. To explore the factor of data length, we vary it as equal to 1000, 2000, 3000, 4000 and 5000 sequentially, The corresponding SVD spectra of these data sets are shown in Fig. 6. One can see that the SVD spectra of different data lengths are almost the same. We note that the computation time of the matrix operation is mainly decided by the size of matrix. To save computation time, we can choose a shorter data length to implement the SVD algorithm and the result is reliable. As to the influence of time delay, we show the results of five different time delays: 0.005, 0.010, 0.015, 0.020, and 0.025 in Fig. 7. Obviously, the feature of exponential decay would be destroyed when the delay is too large. A too long time delay causes the reconstructed trajectory discontinuously and results in a failure. Consequently, the time series used in the SVD analysis must be sampled finely enough. On the other hand, the value of embedding dimensions we used to construct the trajectory matrix is always chosen largely enough to fully expand the SVD spectrum such that both the fast-inclination and the slow-inclination can be included. For a small embedding dimension, as shown in Fig. 8, the SVD spectrum may not be able to reach to the slow-inclination. Thus, when the embedding dimension is small the information of noise level cannot be revealed. We note that although the decay rate is dependent on its own embedding dimension, the feature of exponential decay is always preserved and the noise level is invariant with respect to different dimensions.

In short, if we have chosen appropriate time delay and embedding dimension, the whole SVD spectrum can be obtained from the reconstructed trajectory of a system. The SVD eigenvalue spectrum method works well on detecting the determinism of a complex time series, and there is no ambiguity in determining the "appropriate" ball size in phase space at all.

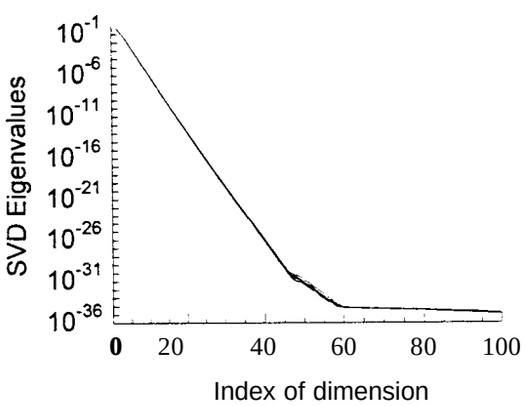

FIG. 6. The SVD eigenvalue spectra for the Lorenz model with different data lengrth 1000, 2000, 3000, 4000, and 5000.

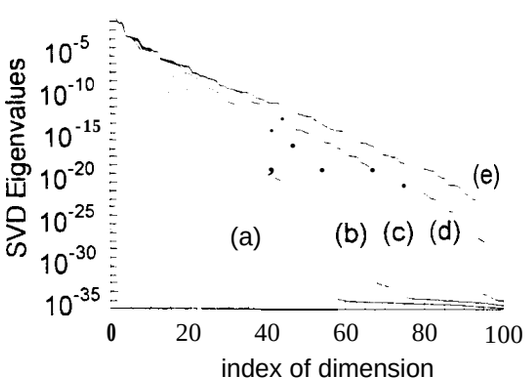

FIG. 7. The SVD eigenvalue spectra for the Lorenz model with different delay time (a) 0.005, (b) 0.010, (c) 0.015, (d) 0.020, and (e) 0.025.

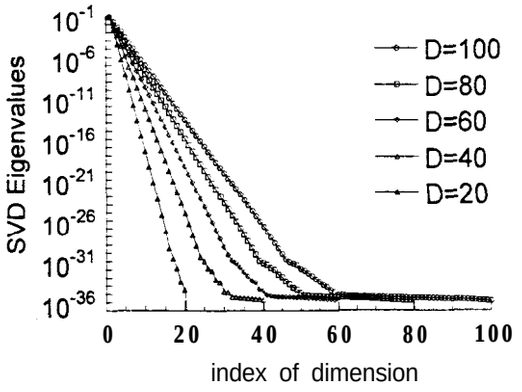

FIG. 8. The SVD eigenvalue spectra for the Lorenz model with different embedding dimension D.

V. Hidden frequency recognition

In this section, we address another applicability of chaos in line with the SVD approach, namely, recognizing the dynamically connected frequency components hidden in the time series. The essential idea has been outlined in the introduction. We will show two methods for the task.

V-l. SVD projection

Let us take the well-known Lorenz model as a numerical illustration. The dynamical equations follow $\frac{dx}{dt} = \sigma(y-x), \frac{dy}{dt} = rx - y - 22$, $\frac{dz}{dt} = xy - bz$, where σ = 10.0, r = 29.0 and b = 2.66. In Fig. 9, the power spectra of the variables x, y and z are presented. One can see that for the variable z a narrow band peaked at the frequency z_1, labeled by a down arrow $\downarrow$, is totally hidden in the power spectrum of the x component. Meanwhile, although the spectra between x and y are similar, there are some frequency components, such as y_1, y_2 and y_3 appeared in the spectrum of y but not in that of the x. This difference is a reflection of the dynamically broken symmetry occurred to the steady state x = y in the Lorenz model. If one only measures the variable x, the frequency z_1, which is important for z, may be missed. Similar consequences also can be made for the frequency components y_1, y_2 and y_3 for y.

As a demonstration of hidden frequency recognition, we choose x as the variable in reconstructing the trajectory matrix. For comparison, we choose the embedding dimension to be exactly three. Typically, the data are taken after transient and the number of data is 40000 with τ = 0.005. This choice ensures the demonstration such that we have a larger Nyquist critical frequency and a smaller frequency interval in the power spectrum. Fig. 10 shows the time series of x, y, and z and the projected variables c_1, c_2, and c_3. Practically, we may neglect c_3 since it is extremely small. The corresponding power spectra of two reconstructed projected variables c_1, and c_2 are shown in (a) and (b) of Fig. 11. This is the result when we use the variable x for the reconstruction. The use of the other variables

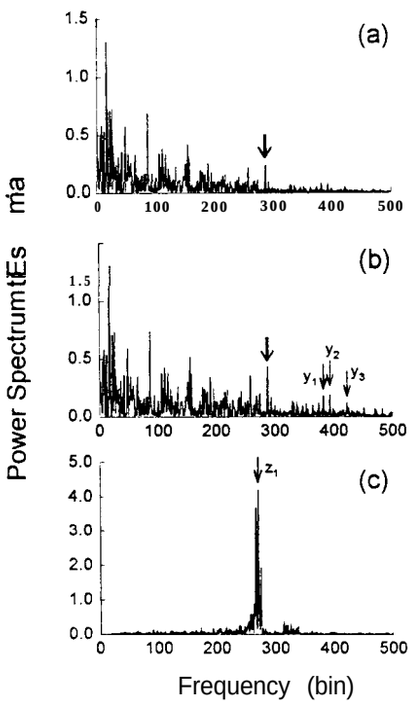

FIG. 9. Power spectra of the Lorenz model for the three variables, (a) x, (b) y, and (c) z, where the parameters $\sigma = 10.0$, $r = 29.0$ and $b = 2.66$.

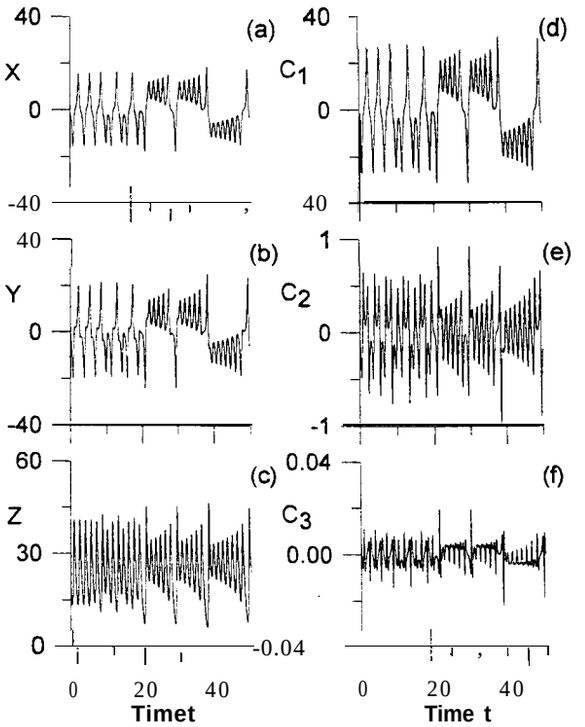

FIG. 10. Time series of the Lorenz model for the variable (a) x, (b) y, and (c) z. The SVD projected variables c_1, c_2, and c_3 are shown in (d), (e) and (f) respectively. The parameter values are the same as those of Fig. 9.

in reconstruction will result in the same fashion. We note that the projected variable c_i (here $i = 1,2,3$) have been defined in the decreasing order by their SVD eigenvalues. It is important to note that the power spectrum of the first projected variable, c_1, is essentially the same as that of the variable chosen in reconstruction.

Next we turn the attention to the spectrum of second projected variable, c_2. The hidden frequency z_1, can be traced out as marked by the down arrow $\downarrow$ shown in Fig. 11(b). One can see that the spectra of z and c_2 are different, though the main frequency peaks are similar. Since c_2 is a projection variable of the trajectory matrix reconstructed from x, its spectrum components originate essentially from x and, implicitly, also from y and z. Indeed, the hidden frequency components y_1, y_2 and y_3 could be found in the spectrum of c_2. Let us label the principal frequency component of c_2 by the down arrow $\Downarrow$. It can be found that this frequency component also appears in the spectra of x and y (see Fig. 9). After carefully identifying every spectrum component, we have found that the spectrum of

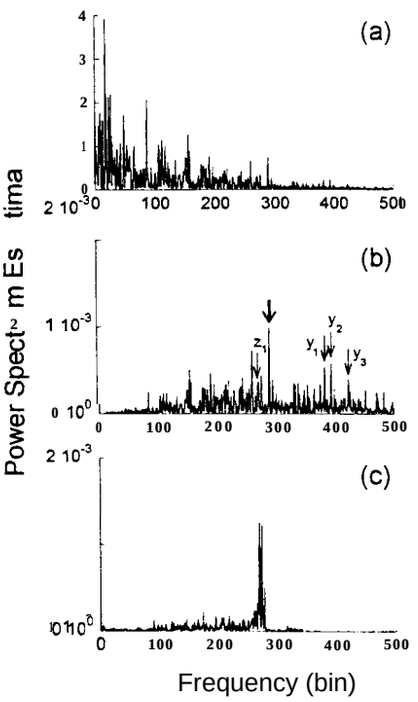

FIG. 11. Power spectra of the SVD projected variable (a) c_1, (b) c_2 and the quantity L, for the Lorenz model. (see text).

c_2 contains the principal components of two spectra of y and z. This shows how well the SVD projection works.

V-2. Rescaled derivative

Although the spectrum of second projected variable c_2 contains the principal components of two spectra of y and z as shown above, there also appears a lot of other frequencies with similar powers. Therefore, we suggest to use another approach as an improvement. Since the main concern is the frequency component, we try to rescale every $c_i(k)$ within the interval [0, 1] and renamed them as $r_i(k)$. The oscillation character of $c_i(k)$ is expected to occur to $r_i(k)$ with different spectral weighting. Next, we calculate a quantity $L(k) = \sum_{i=1}^{d} |r_i(k \text{ t } 1) - r_i(k)|$. This quantity is effectively a distance quantity for the time derivative, $\frac{dr_i}{dt} \approx r_i(k+1) - r_i(k)$. A oscillation character of $r_i(k)$ is also expected to occur to the time derivative, $r_i(k+1) - r_i(k)$. The Lorenz model is reanalyzed. The result is shown in Fig. 10(c). We emphasize that we use the variable x for reconstruction and then after the SVD projection, every c_i is rescaled. One can see that the power spectrum of L(k) corresponds to z very well. The extension to other models, such as the Rossler model and the hyperchaotic Rossler model, have been verify [14].

Let us make a brief summary, we give up choosing the "appropriate" ball size in the

phase space. In contrast, we introduce the SVD algorithm to identify the hidden frequencies. The results shown above indicate that the SVD method can work well on recognizing the frequencies hidden in a scalar time series. We have demonstrated two different schemes in cat ching hidden frequency components. In practice, one can utilize these two schemes together to pick up several main hidden frequency components.

VI. Experimental exploration

It is important to have real experiments as a demonstration. Here we present the diode resonator systems with three different kinds of noises, namely, (1) the observational noise, (2) the additive dynamical noise, and (3) the multiplicative dynamical noise, to show the interplay between the nonlinear deterministic structure and a variety of noises, paying special attention on determinism test.

VI- 1. Observational noise

The diode resonator system with an observational noise configuration is shown in Fig. 12(a), which is a series circuit with a diode (1N5402), an inductor (1.0 H) and a resistor (6.8 KΩ) modulated by a sinusoidal signal. This diode resonator has been used for the demonstration of various chaotic phenomena [18]. Here we use two HP33120A function generators to generate the sinusoidal modulation and the Gaussian noise. The standard deviation of the noise source is $A_N/10$, where A_N is the noise amplitude from the generator. The output voltage $V_{out}\sim$ 1.0 Vpp is the difference voltage across the resistor added with the Gaussian noise with the help of an operation amplifier LF353. Clearly, this configuration typically simulates the case of observation noise. Without the loss of generality, the amplitude and the frequency of sinusoidal modulation are fixed at 5.0 Vpp (Vpp: peak-to-peak voltage) and 15.0 KHz, respectively, at which without the noise configuration the system is chaotic. [19]

The output data V_{out} *are* analyzed by using the SVD spectrum. The sampling rate used for data acquisition is 500 KHz. We usually take the data length 2000. With such a modulation voltage, A_N is constrained to below 9 Vpp due to the power limitation of operation amplifier. We choose seven values of noise amplitude: 0.1 Vpp, 0.5 Vpp, 1.0 Vpp, 2.0 Vpp, 3.0 Vpp, 4.0 Vpp, and 5.0 Vpp. In other words, the standard deviations of the noise source σ are 0.01 Vpp, 0.05 Vpp, 0.1 Vpp, 0.2 Vpp, 0.3 Vpp, 0.4 Vpp, and 0.5 Vpp and the ratio R_S are 0.01, 0.05, 0.1, 0.2, 0.3, 0.4, and 0.5. The results of the SVD analysis are shown in Fig. 12(b). As expected, the SVD spectrum displays an exponential decay and a slow inclination. One can see that there appears kink structure indicated by arrow. These kinks reflect the intrinsic dynamical nature of the diode resonator.

VI-2. Additive dynamical noise

For the case of additive dynamical noise, another circuit is constructed. The systematic diagram is shown in Fig. 13(a). We use the operational amplifier, LF353, to sum the sinusoidal signal and the Gaussian noise. This summation is further used to drive the diode resonator. Thus, the noise is playing a role of dynamical noise. Again, the amplitude of the driving sinusoidal is 5.0 Vpp and the frequency is 15.0 KHz. The conditions of data

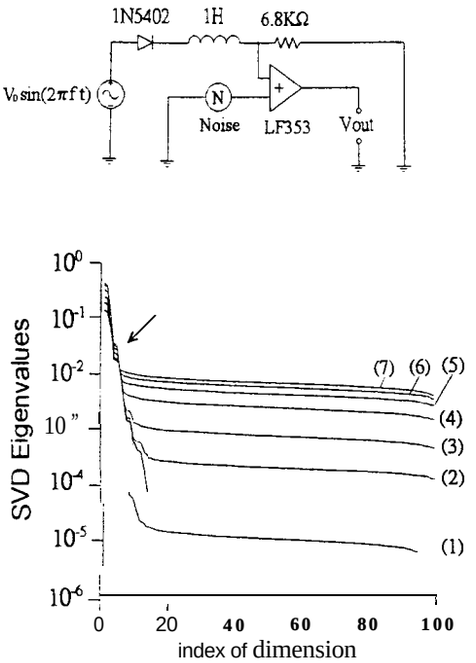

FIG. 12. (a) The diode circuit with a observational noise added to the voltage output of the resister. (b) The SVD eignevalue spectra. The amplitude of observational noises are (1) 0.1 Vpp, (2) 0.5 Vpp, (3) 1.0 VPP, (4) 2.0 Vpp, (5) 3.0 Vpp (6) 4.0 Vpp, and (7) 5.0 Vpp. The amplitude and frequency of driving sine signal are 5.0 Vpp and 15 KHz respectively. The time series is sampled at 500 KHz by measuring the voltage amplitude of the resister. Data length is 2000.

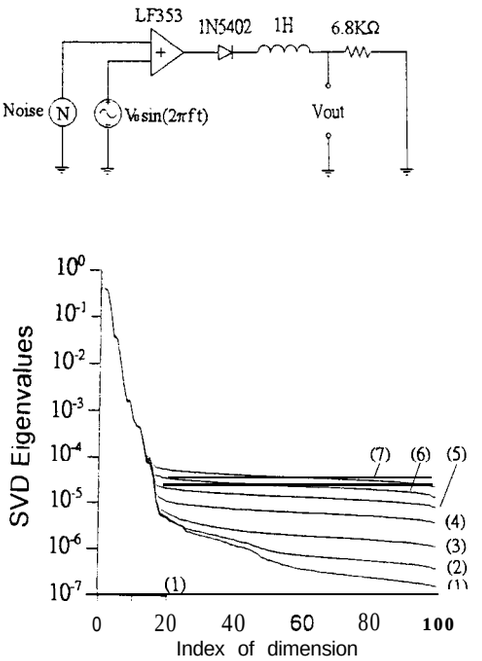

FIG. 13. (a) The diode resonator driven by the sum of a sine and stochastic signal. (b) The SVD eignevalue spectra. The amplitude of simple dynamical noises are (1) 0.1 Vpp, (2) 0.5 Vpp, (3) 1.0 Vpp, (4) 2.6 Vpp, (5) 3.0 VPP (6) 4.0 Vpp, and (7) 5.0 Vpp.

acquisition are the same as that mentioned above. The experimental data is obtained by measuring the voltage amplitude across the resistor. We had also chosen seven amplitudes of noise to perform the analysis, namely, 0.1 Vpp, 0.5 Vpp, 1.0 Vpp, 2.0 Vpp, 3.0 Vpp, 4.0 Vpp, and 5.0 Vpp. As one can see in Fig. 13(b), the feature of the SVD spectrum, the exponential decay and the noise level, remains. Meanwhile, the kinks still occur.

VI-3. Multiplicative dynamical noise

Let us turn to consider another case, Fig. 14(a) shows the experimental setup of a diode resonator system with multiplicative dynamical noise. Through a multiplier IC,

AD632, the generated noise is multiplied by the output V_{out} to produce multiplicative dynamical noise. The multiplicative dynamical noise is further added with the sinusoidal modulation by LF353, and then used to drive the circuit. This forms a feedback loop actually. With such a modulation voltage, A_N is constrained to below 9 Vpp due to the voltage limitation of the operation amplifier/multiplier. The amplitude and the frequency of sinusoidal modulation, the sampling rate and the data length used for data acquisition are all the same as those mentioned above.

Referring to Fig. 12(b) and Fig. 13(b), the stochastic responses of the case of multiplicative dynamical noise are different, as comparing with Fig. 14(b). Although there also appears exponential decay with some kink structures, indicated with the down arrows ↓, the decay rates are no longer to be the same when different noise strength is varied. As the noise amplitude goes up, the decay rate drops more rapidly.

In Fig. 15, for the observational noise case, the result of the smaller noise ratio consists with Eq. (7). As the noise ratio increases to 1, the deviation appears as mentioned in

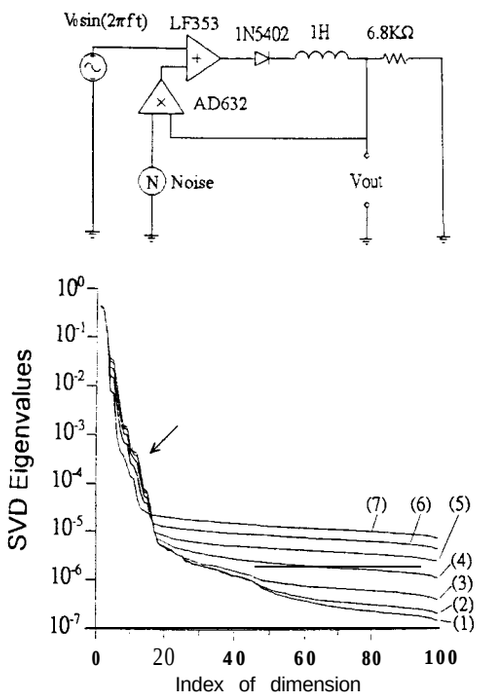

FIG. 14. (a) The diode resonator driven by the sum of sine wave and the variable-dependent noise. (b) The SVD eignevalue spectra. The amplitude of multiplicative variable noises are (I) 0.1 Vpp, (2) 0.5 Vpp, (3) 1.0 Vpp, (4) 2.0 Vpp, (5) 3.0 Vpp, (6) 4.0 Vpp, and (7) 5.0 Vpp.

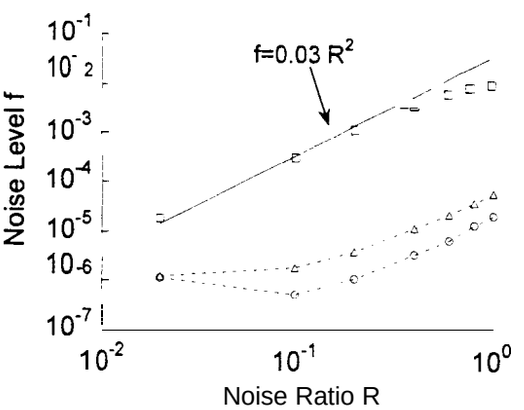

FIG. 15. The noise ratio R versus the noise level f. The Square points are the experimental data for observational noise. The triangle points are the experimental data for additive noise. The circle points are the experimental data for multiplicative noise. The line is $f = 0.03\ R^2$.

Sec. IV(B). However, for the additive dynamical noise and the multiplicative noise, we note that as noise amplitude increases, the noise ratio and the noise level could not follow Eq. (7). In short, testing determinism based on the SVD scheme can be operated very well in the observational noise situation of real experiment but does not for the others.

VII. Conclusions

We have shown that the exponential decay of the SVD spectrum is due to the intrinsic correlation of the chaotic time series. It has also been studied that the data length, the time delay, and the embedding dimension influence in the SVD spectrum method. A variety of time series originated from different generation processes has been employed to show the validity of the SVD analysis. Furthermore, three different kinds of circuit systems have been utilized to explore the SVD analysis in testing determinism. Although the kinds of noise are different, the SVD spectra still have the exponential decay and the noise level. It is worthwhile to note that the SVD method gets rid of the conception of an "appropriate" ball size in phase space. Hence, there is no ambiguity in judging which ball size could be appropriate.

The criterion based on the SVD spectrum can be a flexible method, which is good for testing the determinism, estimating the noise strength, and recognizing the hidden frequency components in a time series, which we presumed that it is generated from a continuous-time dynamical system. Unfortunately, the SVD analysis presented here could not be extended to the discrete dynamical system. This is also true for the discrete data reduced from the Poincare section. This defect urges the development of a similar analysis for the discrete data. This is a nontrivial task and work to this goal is on the progress. Although the noise estimate works very well for small noise strength, there remains inconsistency in the case of strong noise. Thus, how to derive a suitable estimate is still a difficult problem with current interest. On the other hand, though we have derived two working criteria to deduce the hidden frequency components effectively, there remain no general applicable rules to deal this inverse problem.

Acknowledgment

This work is partially supported by the National Science Council, Taiwan ROC under the project number: 86-2112-M006-016. J.-L. Chern thanks R.-R. Hsu and H.-T. Su for useful discussion. Thanks also extend to I.-M. Jiang.

References

[1] G. Sugihara and R. M. May, Nature (London) 344, 734 (1990).
[2] D. T. Kaplan and L. Glass, Phys. Rev. Lett. 68, 427 (1992).
[3] R. Wayland, *et* al., Phys. Rev. Lett. 70, 580 (1993).
[4] L. W. Salvino and R. Cawley, Phys. Rev. Lett. 73, 1091 (1994).
[5] D. E. Newland, in An Introduction *to* Random *Vibrations, Spectral* and *Wavelet* Analysis, 3nd. Ed. (Longman Scientific and Technical, England, 1993) and references therein.
[6] G. J. Ortega, Phys. Lett. A209, 351 (1995); Phys. Rev. Lett. 77, 259 (1996).
[7] D. S. Broomhead and G. P. King, Physica D20, 217 (1986).

[8] A. M. Albano, et al., Phys. Rev. **A38**, 3017 (1988).
[9] R. Brown, P. Bryant, and H. D. I. Abarbanel, Phys. Rev. A43, 27 (1991).
[10] R. Stoop and J. Parisi, Physica D50, 89 (1991).
[11] R. Cawley and G. H. Hsu, Phys. Rev. A46, 3057 (1992); Phys. Lett. **A116**, 188 (1992).
[12] T. Saucer, Physica D58, 193 (1992).
[13] J.-S. Lih, *et* al., Europhys. Lett. 40, 7 (1997).
[14] J.-L. Chern, *et al.,* Phys. Lett. A238, 134 (1998).
[15] T. Sauer, J. A. Yorke, and M. Casdagli, J. Stat. Phys. 65,579 (1991); F. Takens, in *Dynamical System and* Turbulence, eds. D. A. Rand and L. S. Young (lectrure notes in mathematics, vol. 898; Springer, Berlin, 1981) pp. 366-381.
[16] D. Pierson and F. Moss, Phys. Rev. Lett. 75, 2124 (1995).
[17] J. Theiler, *et al.,* Physica D58, 77 (1992).
[18] H.-J. Li and J.-L. Chern, Phys. Rev. E54, 2118 (1996).
[19] J.-S. Lih, *et al.,* Europhys. Lett. 42, 383 (1998).